Supporting Information

The Role of Solvent-Additive Processing in High Performance Small Molecule Solar Cells

Louis A. Perez,[†,‡,#] James T. Rogers,[†,‡,#] Michael A. Brady,[†,‡,#] Yanming Sun,[†] Gregory C. Welch,[†,⊥] Kristin Schmidt,[ø] Michael F. Toney,[ø] Hiroshi Jinnai,[Ω] Alan J. Heeger,[†,‡,§,#], Michael L. Chabinyc,[†,‡,#] Guillermo C. Bazan*,[†,‡,§,#], and Edward J. Kramer,*[‡,||,#]

[†]Center for Polymers and Organic Solids, [#]Materials Research Laboratory, [‡]Departments of Materials, [§]Chemistry and Biochemistry, and [||]Chemical Engineering, University of California, Santa Barbara, California 93106, United States

[ø]Stanford Synchrotron Radiation Lightsource, SLAC National Accelerator Laboratory, Menlo Park, California 94025, United States

[Ω]Institute for Materials Chemistry and Engineering (IMCE), Kyushu University, CE80, Kyushu University, 744 Motooka, Nishi-ku, Fukuoka 819-0395, Japan

1. Azimuthally integrated GIWAXS of *p*-DTS(PTTh$_2$)$_2$:PC$_{71}$BM

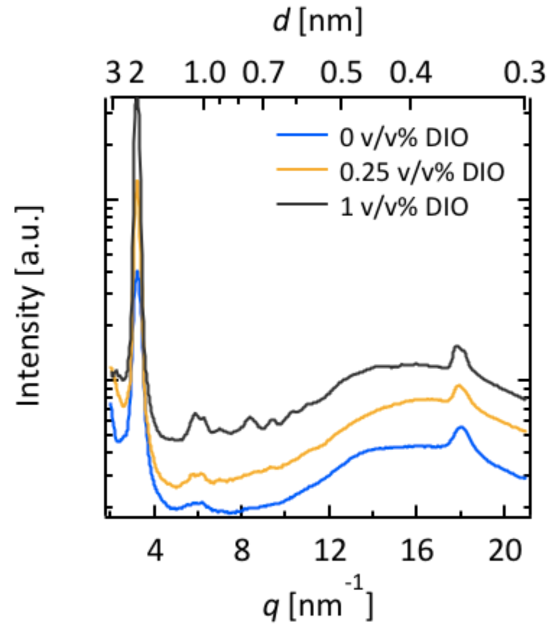

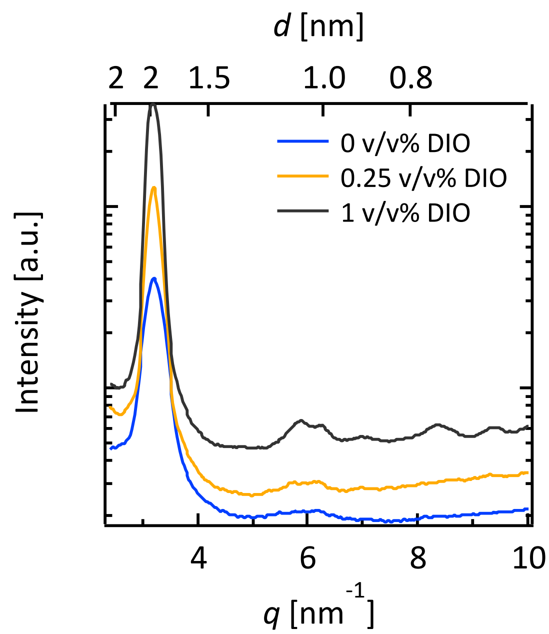

Figure S1. Azimuthally integrated intensity ($q = ((q_{xy})^2+(q_z)^2)^2$) line cuts over all orientations of *p*-DTS(PTTh$_2$)$_2$:PC$_{71}$BM with 0, 0.25, and 1.0 v/v% DIO added to the film casting solution (top) and a close-up of the low *q* region (bottom). There is little difference observed between 0 and 0.25 v/v% DIO, with only two main strong reflections at $q \sim 3.5$ and 18 nm^{-1} which correspond to the unit cell axis and π-π stacking peak, respectively. When 1 v/v% DIO is added to the casting solution, more Bragg reflections appear, indicating that higher DIO concentrations increase *p*-DTS(PTTh$_2$)$_2$ crystallite quality or perfection. The curves are shifted vertically for clarity.

2. Electron energy loss spectroscopy (EELS) of *p*-DTS(PTTh$_2$)$_2$ and PC$_{71}$BM

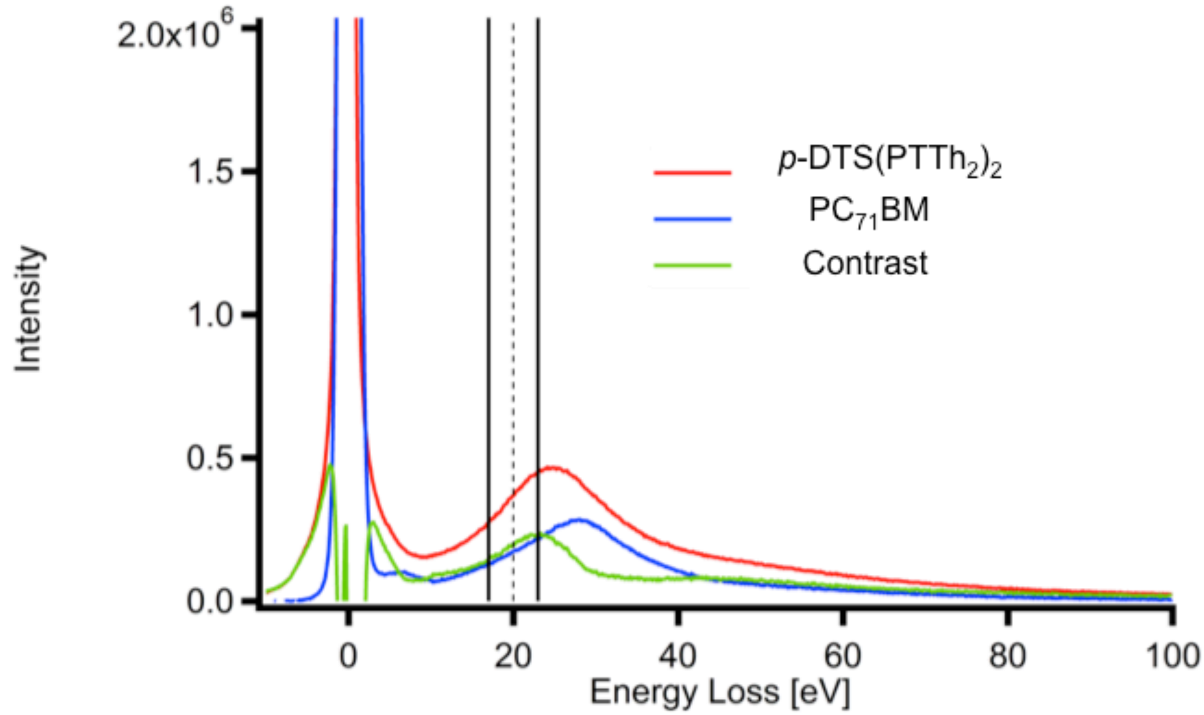

Figure S2. Electron energy loss spectroscopy (EELS) of *p*-DTS(PTTh$_2$)$_2$ and PC$_{71}$BM and contrast between them (*p*-DTS(PTTh$_2$)$_2$ - PC$_{71}$BM). The black vertical lines indicate the energy loss regime to achieve maximum contrast between the two moieties for energy filtered transmission electron microscopy (EF-TEM).

3. High resolution X-ray reflectivity (HR-XRR) of *p*-DTS(PTTh$_2$)$_2$:PC$_{71}$BM

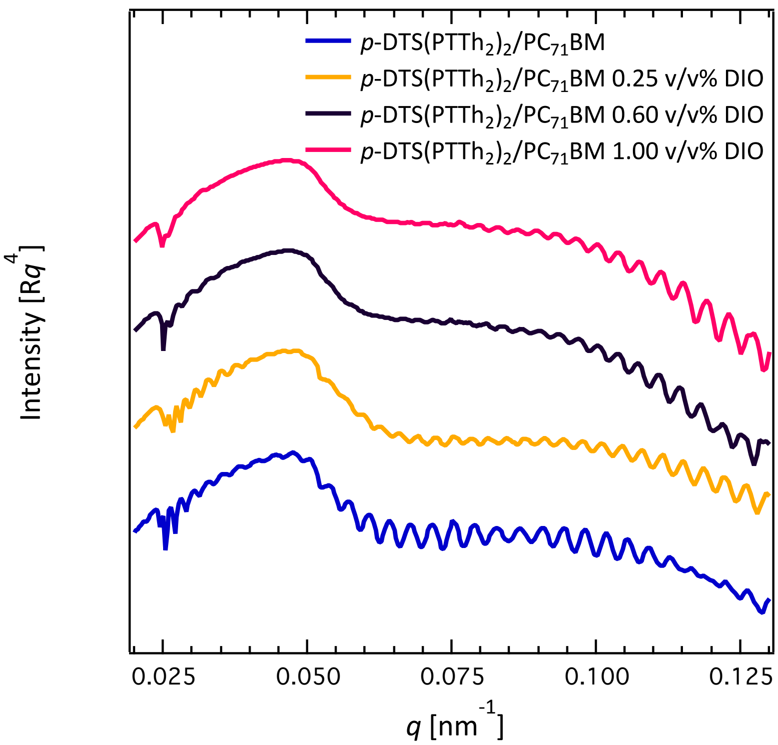

Figure S3. High resolution X-ray reflectivity of *p*-DTS(PTTh$_2$)$_2$:PC$_{71}$BM with different DIO loadings.

4. In-plane intensity corrected GISAXS line-cuts of *p*-DTS(PTTh$_2$)$_2$:PC$_{71}$BM

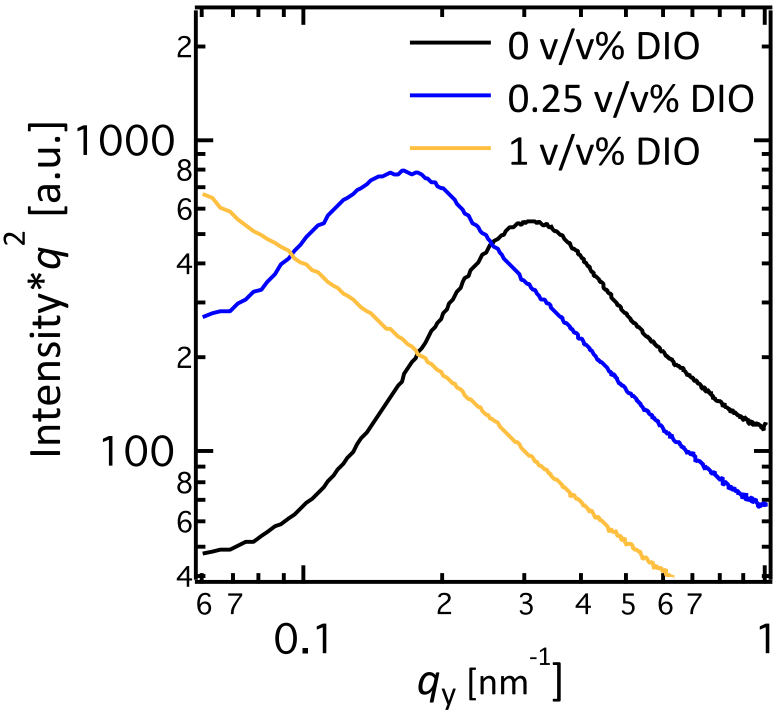

Figure S4. Intensity corrected grazing incidence small-angle X-ray scattering (GISAXS) in-plane (q_y) line cuts, taken from the scattering patterns in **Figure 5**, of *p*-DTS(PTTh$_2$)$_2$:PC$_{71}$BM with 0, 0.25, and 1.0 v/v% DIO added to the film casting solution.

5. Cake segment-sector plot of π-π stacking region in *p*-DTS(PTTh$_2$)$_2$:PC$_{71}$BM 1 v/v% DIO

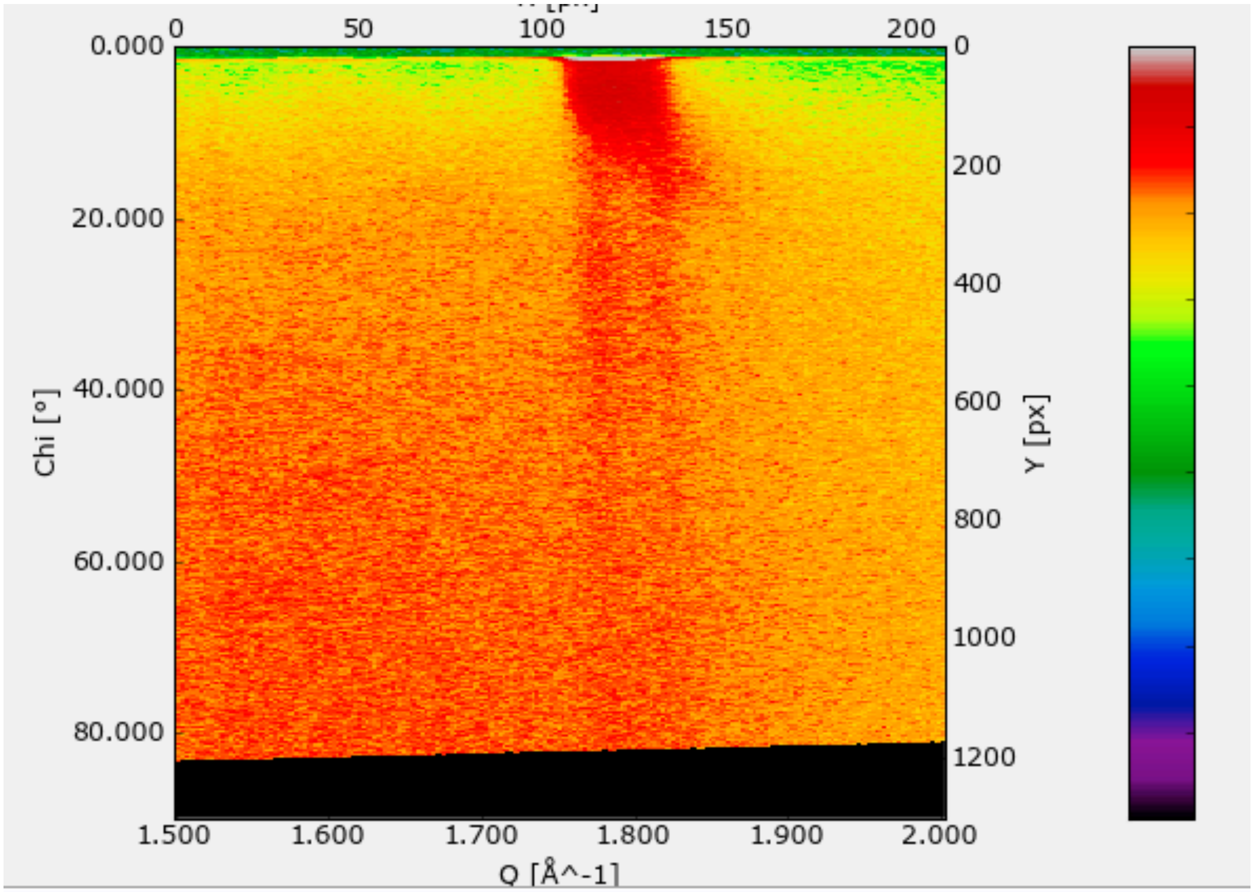

Figure S5. Close-up of the π-π stacking peak splitting seen in 1 v/v% DIO treated *p*-DTS(PTTh$_2$)$_2$:PC$_{71}$BM thin films.

6. EF-TEM and EF-TEMT measurements and data work-up

Electron tomography was performed using a JEOL JEM-2200FS microscope that combines a 200kV field emission gun and an in-column energy filter (Omega Filter). Images were taken at 1° increments over a range of ±68° with an image acquisition time of 2 seconds at each step. In order to enable proper image registration for tomographic reconstruction, 5 nm diameter gold nanoparticles were applied to the sample surface via drop casting from dilute aqueous solution prior to imaging. After image acquisition, a manual realignment of the images was performed by utilizing the gold particles as fiduciary markers. The necessary image shifts, required to bring the images into registration, were recorded using this technique, and then the gold markers were "removed" from the images by replacing the dark pixels composing the markers with intensity values equal to the average value of all of the other non-fiduciary pixels in the image. A similar procedure was used to reduce the intensity of spurious high (low) intensity pixels in each of raw 32bit tilt-series images. High (low) intensity pixels above (below) an intensity that is six standard deviations above (below) the mean determined by taking a histogram of the entire tilt-series images were reduced (increased) to the value of the intensity six standard deviations above (below) the mean of the distribution (i.e. "artificially binned"). The modified images (with the markers removed and the high/low intensity pixels "artificially binned") were then converted to 16bit images and used as the input data for the tomographic reconstruction software.

The 3 videos included in the Supporting Information are of *p*-DTS($PTTh_2$)$_2$:$PC_{71}BM$ with 0, 0.25, and 1 v/v% DIO added to the casting solution. The videos are loops that start with views from the top of the film and gradually work its way to the bottom, and then back to the top of the film. The dark markers seen at the beginning or end of each loop are from the gold markers as described previously.